Paper 268

Gravity Effect on the Catastrophic Dynamic Response of Strain-Hardening Multi-story Frames

by

R. Tananbashi, T. Nakamur, and S. Ishida

Discussed by Dr. Franklin Y. Cheng, Associate Professor of Civil Engineering, University of Missouri, Rolla, Missouri 65401, USA

The P-Δ effect considered in the paper seems due to static axial load only. For tall buildings, longitudinal inertia forces (due to vertical ground motion) and the girder shears transfered to columns may be significant on P-Δ effect. The writer will appreciate their comments why they have neglected these effects.

Paper 268, "Gravity Effect on the Catastrophic Dynamic Response of Strain-Hardening Multi-story Frames", by R. Tanabashi, T. Nakamura, and S. Ishida

Prepared discussion by Dr. Franklin Y. Cheng, Associate Professor of Civil Engineering, University of Missouri, Rolla, Missouri 65401, USA

The P-Δ effect considered in the paper seems due to static axial load only. For tall buildings, longitudinal inertia forces (due to vertical ground motion) and the girder shears transferred to columns may be significant on P-Δ effect. The writer will appreciate their comments why they have neglected these effects.

Authors (In written reply):

The authors are grateful to Dr. Cheng for offerring them a chance to present some further details of the numerical method of the present paper.

(1) In dealing with a plane frame as representing the in-plane behavior of a set of parallel frames of the original three-dimensional frame, it is considered appropriate to assume that the effect of the inertia forces transmitted by the orthogonal out-of-plane beams can be well simulated by the lumped masses at the joints. The inertia forces of the distributed masses of columns and those transmitted by the in-plane beams may be either treated by the consistent mass matrix technique (resulting in a variable mass matrix in this case) or simulated by those of some appropriate lumped masses. In the present paper, the mass matrix has been formed by assuming lumped masses at joints as has been stated as the third assumption in Section 2.

(2) An apparent understanding of Dr. Cheng's discussion, therefore,is that the longitudinal inertia forces due to the lumped masses at joints subjected to vertical ground motion and the additional column axial forces due to varying girder shears should be incorporated in the PΔ analysis. As for this point, the authors would like to point out that all the informations related to joints, member ends and element ends have been expressed in terms of horizontal, vertical and rotational coordinates as shown in Fig.2, 3 and 4. Consequently, the longitudinal inertia forces due to the lumped masses have all been included in the terms $[M]\{\Delta\ddot{u}\}$ and $[M]\{\Delta\ddot{u}_g\}$ in Eq.14. Varying girder shears are automatically transferred to columns through the vertical coordinates defined at girder ends and then transformed to element PΔ-terms of columns. The second term of the right side of Eq.8 and the third term of the right side of Eq.9 include such terms. Therefore the PΔ effects due to varying girder shears have all been taken into account in the present theory.

(3) If Dr. Cheng's discussion is to raise the question regarding the effect of longitudinal wave propagation in columns due to the distributed masses and of additional vertical inertia forces due to the distributed masses along girders, the authors would like to mention that these effects have been neglected in the present analysis because of the following reasons : (i) The order of distributed masses along columns are considerably small compared to that of the slabs and carried masses and therefore the significant portion of the effect of longitudinal wave propagation in columns of multi-story frames can be taken into account by the lumped masses at joints ; (ii) the effect of "additional" vertical inertia forces in girders which is due to the difference between the distributed and lumped mass systems, can be incorporated in the analysis more properly even with lumped masses provided that the connectivity between slabs, cross-beams and girders is specified or assumed and that some additional lumped masses are placed on girders, but it has simply been left for further study from the present first step of the numerical analysis for clarifying the "overall" dynamic behaviors of frames.

EFFECT OF GRAVITY LOADING ON THE EARTHQUAKE RESPONSE OF COOLING TOWERS

by

V. I. Weingarten[I], S. F. Masri[II], M. Lashkari[III], and K. Kahyai[IV]

SYNOPSIS

The natural frequencies and mode shapes of a clamped-clamped and clamped-free hyperboloidal shell were determined analytically and experimentally. Good correlation was obtained between the experimental and analytical results. The effect of dead weight loading on the natural frequencies of three arbitrarily selected typical cooling towers was determined. The natural frequencies of the 1000 foot cooling tower were lowered considerably by the inclusions of dead weight loading. The dynamic response of the cooling tower was also determined. An experimental investigation of the response of a hyperboloidal shell subjected to a harmonic loading applied through a rigid plate indicated that the shell responded in the beam mode as well as other modes of the shell. The San Fernando earthquake of 1971 was applied as a dynamic load to the 1,000 foot cooling tower and the deflection response was calculated by considering the strong motion portion of the acceleration record and approximating the ground acceleration as a stationary random process. The mean square response of the deflection of the cooling tower was found to be much larger if the dead weight loading is considered.

INTRODUCTION

Hyperboloidal shells of revolution are used as cooling towers to dissipate low density heat from electrical and chemical plants. Until the collapse of the Ferrybridge cooling towers in England in 1965, very little work had been done on determining the dynamic characteristics of cooling towers. Recently a number of papers (1-4) have considered this problem. None of the investigations, however, have accounted for the effect of dead weight loading on the natural frequencies and earthquake response of hyperboloidal shells of revolution.

The present investigation determines the natural frequencies of hyperboloidal shells subjected to dead weight loadings. Sanders' (5) thin shell equations, in conjunction with a curved meridian frusta finite element, were used to formulate a linear eigenvalue problem to determine the natural frequencies of the shell. The dead weight loading was con-

[I] Prof. of Civil Engrg., Univ. of Southern California.

[II] Assoc. Prof. of Civil Engrg., Univ. of Southern California.

[III] Asst. Prof. of Mech. Engrg., Aryamehr Univ. of Technology.

[IV] Student, University of Southern California.

sidered by developing a shell geometric stiffness matrix. The mean square response of the cooling tower to earthquake excitation considering the effect of dead weight loading, was computed by approximating the strong motion segment of the acceleration record as a stationary random process, as described in (2).

An experimental program was carried out in conjunction with the analysis. Holographic interferometry was used to determine the natural frequencies and mode shapes of a clamped-clamped and clamped-free hyperboloidal shell of revolution. The experimental data are in good agreement with the analysis. The dynamic response of the hyperboloidal shell to harmonic loading was also obtained experimentally. A rigid plate was attached to the top of the shell as shown in Fig. 1 and a sinusoidal force was applied to the rigid plate by an electrodynamic shaker. Results from the experiment indicate that the shell responds at the natural frequencies of all the low frequency shell modes. This is in contradiction to the predictions obtained by the normal mode method for a perfect shell. The perfect hyperboloidal shell should respond only in the beam mode for the forcing function applied.

VIBRATION ANALYSIS

The finite element method was used to determine the modes and frequencies of the hyperboloidal shell of revolution. A more detailed description of the analysis and computer program can be found in (4). The analysis was based on thin shell theory. The strain displacement relations derived by Sanders (5) for moderate bending were used in the evaluation of the shell strain energy. The finite element model chosen to represent the shell of revolution was formed by a series of frusta with curved meridians. Each frustum is bounded by two "nodal circles" or "nodes", so that the displacements of the continuous shell are described by the displacements of the nodes. Four degrees of freedom were assumed at each node. The displacement field within each element was expressed by Fourier series in the circumferential direction and by higher order Hermitian polynomials along the meridians. In view of the axisymmetric nature of the problems and its linearity, each Fourier component was considered separately. To describe the mathematical form of the eigenvalue problem that represents the state of shell free vibrations, Hamilton's principle was used leading to the following matrix equation in terms of the generalized coordinates,

$$\left\{\frac{d}{dt}\left(\frac{\partial T}{\partial \dot{q}}\right)\right\} + \left\{\frac{\partial U}{\partial q}\right\} - \left\{\frac{\partial W}{\partial q}\right\} = \{0\} \qquad (1)$$

where T and U are the shell kinetic and strain energies, respectively. The term W denotes the work done by the dead weight loading. Substitution of U, W and T into Eq. 1 yields the eigenvalue relation from which the shell natural frequencies and mode shapes are determined, namely

$$[K]\{q\} + [K_g]\{q\} = \omega^2 [M]\{q\} \tag{2}$$

where $[K]$, $[K_g]$ and $[M]$ represent the assembled stiffness, geometric stiffness and inertia matrices of the overall shell with the appropriate boundary conditions imposed.

A large capacity finite element computer program was written to perform the computations required to first determine the stresses in the shell due to the dead weight loading and then determine the natural frequencies and mode shapes defined by Eq. 2. The solution for the initial load condition required the decomposition of a large banded matrix by the Cholesky square root method. The Sturm sequence technique was used to determine the eigenvalues and eigenvectors of the banded matrices appearing in Eq. 2.

DYNAMIC RESPONSE

Forced Vibration

The dynamic response of the cooling tower including the effects of gravity, follows the presentation given in (2). Using the method of spectral representation (6), each of the three spatial displacements u, v, and w may be expressed by the expansion

$$u = \sum_{m=1}^{\infty} q_m(t)\, U_m \cos n\theta \; ; \; v = \sum_{m=1}^{\infty} q_m(t)\, V_m \sin n\theta$$

$$w = \sum_{m=1}^{\infty} q_m(t)\, W_m \cos n\theta \tag{3}$$

where $q_m(t)$ is the generalized coordinate for mode m representing the time-dependent aspects of motion, and the dependent variables U_m, V_m, and W_m are associated with the m^{th} mode of free vibration that occurs with frequency ω_m.

By making use of the orthogonality condition for the modes of free vibration of the shell, it can be shown (6) that

$$\ddot{q}_m + 2\zeta_m \omega_m \dot{q}_m + \omega_m^2 q_m = \frac{P_m(t)}{M_m} \tag{4}$$

where $\zeta_m \equiv$ ratio of critical damping in mode m

$\omega_m \equiv$ natural frequency of mode m

$$P_m(t) \equiv \int\int (p_1 U_m + p_2 V_m + p_3 W_m)\, R\, d\theta\, ds \tag{5}$$

$$M_m \equiv \rho h \int\int (U_m^2 + V_m^2 + W_m^2)\, R\, d\theta\, ds \tag{6}$$

and p_1, p_2, and p_3 are the components of the excitation in the direction

of u, v, and w. For the finite element method, the integrals are replaced by summation.

Response to Earthquake Excitation

An earthquake ground motion can be represented by a horizontal component of ground acceleration and will induce horizontal inertia forces to act on the shell. If it is assumed that the base of the shell is completely rigid, then the only allowable circumferential base deformation is the beam mode n = 1.

With the horizontal inertia force loading, the generalized force $P_m(t)$ and the generalized mass M_m can be found from Eq. 5 and Eq. 6, respectively. Then Eq. 4 can be solved, and the time history of the response can be obtained from Eq. 3.

For reasonable accuracy in determining the transient response it is necessary to consider a large number of modes and frequencies. To evaluate the response at short time increments, the "exact" solution of this problem by means of digital computers is quite expensive, even when employing efficient codes.

An alternate approach to obtaining the response to earthquake induced ground motion is to represent the strong motion duration of the earthquake (typically, 15-50 sec.) by a segment of a stationary random process. Tajimi (7) has shown that for such processes, the ground acceleration power spectral density (psd) can be approximated by

$$S_{\ddot{x}_g}(\omega_m) = \frac{8\,H}{\left[1+(2H)^2\right]} \cdot \frac{\xi\left[1+(2H\xi)^2\right]}{\left[(1-\xi^2)^2+(2\xi H)^2\right]} \cdot \frac{\sigma^2(\ddot{x}_g)}{\omega_m} \qquad (7)$$

where $\xi \equiv$ frequency ratio $= \omega_m/\omega_g$, where ω_g is a characteristic ground frequency, $(\omega_g/2\pi \approx 2.5$ Hz.);

$H \equiv$ characteristic damping ratio of ground, ≈ 0.65;

$\sigma^2(\ddot{x}_g)$ = earthquake mean-square value.

By substituting the horizontal inertia forces into Eq. 5, the generalized force $P_m(t)$ can be related to the ground acceleration by

$$P_m(t) = \rho\, h\, m_m\, \ddot{x}_g(t) \qquad (8)$$

where m_m is the m^{th} modal participation factor. Then the psd of $P_m(t)$ can be related to that of $\ddot{x}_g(t)$ by

$$S_{P_m}(\omega_m) = (\rho\, h\, m_m)^2\, S_{\ddot{x}_g}(\omega_m). \qquad (9)$$

Assuming that the damping of the shell is slight and that the response in each mode is confined mainly to the resonant peak, then with

the aid of Eq. 7, the mean square of the generalized response in the m^{th} mode is approximately equal to

$$\sigma^2(q_m) = [(\rho h m_m)^2/(8 \zeta_m \omega_m^3 M_m^2)] S_{\ddot{x}_g}(\omega_m) \qquad (10)$$

Assuming no significant cross coupling between modes, the mean square response of the displacements can now be found from Eq. 3.

EXPERIMENTAL PROCEDURE

A hyperboloidal shell of revolution as shown in Fig. 1 was manufactured from 0.034 inch thick 6061-0 aluminum. The geometry of the shell is shown in Figs. 3 and 4. The material properties of the shell were $E = 10 \times 10^6$ psi; $\nu = 0.3$; and $\rho = 0.1$ lb. per in^3. To provide for the clamped support conditions, the shell was placed in a circular groove machined in a 3/4 inch thick aluminum plate as indicated in Fig. 2. The groove was then filled with molten Cerrobend, a low melting point alloy, which was allowed to solidify furnishing the desired fixity. The shell was also painted with flat white paint for a better diffusing surface.

An electromagnet, which was connected to an oscillator and power-amplifier, was used to excite the specimen. A microphone was used to detect the resonances of the shell. A diagram of the experimental set-up appears in Fig. 3. Holographic interferometry was used to determine the shell mode shapes at resonant frequencies. The arrangement used for obtaining time-average holograms of the shell modal patterns are shown in Fig. 4. In the experiment, a helium-neon continuous wave laser accounted for the monochromatic coherent light source. In making the holograms Agfa Gavaet 8E75 glass plates were utilized.

The shell shown in Fig. 1 was also excited by an electrodynamic shaker. The harmonic exciting force was applied to a thick disk attached to the top of the shell. The boundary conditions at the top of the shell resulted in an applied force similar in form to that obtained from base excitation.

RESULTS

Experimental results for the free vibration characteristics of the clamped-clamped and clamped-free hyperboloidal shell of revolution appeared in graphical preliminary form in Ref. 1 but are included in this paper in Figs. 5 and 6 and Tables I and II for completeness. The plotted experimental data given in Figs. 5 and 6 are in good agreement with one another. In Figs. 7 and 8 different modal patterns obtained through holographic interferometry are presented.

The natural frequencies of a ring stiffened hyperboloidal shell considered in (4) were compared with the present finite element analysis in Table III. A comparison of the data indicates good agreement between

the different solution techniques. A number of cooling towers with different geometries were also analyzed. The dimensions of the cooling towers appear in Fig. 9. A plot of the effect of dead weight loading on the natural frequencies of the shell appear in Fig. 10. The dead weight loading has an appreciable effect on the natural frequencies of the tallest cooling tower considered in the analysis.

Results from the normal mode analysis indicate that the cooling tower should respond only in the beam mode if a beam mode forcing function is applied. To verify this prediction an electrodynamic shaker was attached to a rigid top plate in order to apply a beam type forcing function. A frequency sweep through the natural frequencies of the shell indicated that the shell had a significant response in the beam mode and also in modes other than the beam mode. One explanation of these results is that the slight imperfections in geometry of the shell and the small deviation of the end plate from simulating a rigid plate are responsible for exciting resonances other than n=1. This situation is similar to that encountered in the earthquake response of actual cooling towers.

The dynamic response of the cooling tower shown in Fig. 9c subjected to the San Fernando earthquake of 1971 was determined utilizing Eq. 10. A plot of the mean square response of the deflection for one mode and eight modes of the beam mode shape is shown in Fig. 11. Since the experimental results indicate that all modes will probably be excited by the ground motion of an earthquake, the mean square response of the deflection was computed for a number of circumferential wave numbers. These results are also plotted in Fig. 11. The curves shown in Fig. 11 indicate that the rms of the deflection is much larger if the dead weight loading is considered. For the San Fernando earthquake it appears that the response of the cooling tower in circumferential modes other than the beam mode can be significant.

CONCLUSIONS

It has been shown that:

1. By means of holographic interferometry accurate experimental modal data can be obtained to determine the dynamic characteristics of shells of revolution.
2. Dead weight loading has a large effect on the natural frequencies and dynamic response of tall cooling towers.
3. Experimental data indicate that the cooling tower will probably respond in modes other than the beam mode.

Further research in this problem area is still required in order to obtain needed design criteria to predict structural failure of cooling towers subjected to earthquake loading. Future investigations should consider the effects of shell imperfections, base flexibility, and soil-structure interaction on the dynamic response of cooling towers.

ACKNOWLEDGEMENT

This investigation was supported by the National Science Foundation.

REFERENCES

1. Lashkari, M., Weingarten, V. I. and Margolias, D. S., "Vibrations of Pressure Loaded Hyperboloidal Shells," Journal of the Engineering Mechanics Division, ASCE, Vol. 98, No. EM5, Proc. Paper 9230, Oct. 1972, pp. 1017-1030.

2. Abu-Sitta, S. H., and Davenport, A. G., "Earthquake Design of Cooling Towers, "Journal of the Structural Division ASCE, Vol. 96, No. ST9, Proc. Paper 7524, Sept. 1970, pp. 1889-1902.

3. Hashish, M. G., and Abu-Sitta, S. H., "Free Vibration of Hyperbolic Cooling Towers, "Journal of the Engineering Mechanics Division, ASCE, Vol. 97, No. EM2, Proc. Paper 8037, Apr. 1971, pp. 253-269.

4. Lashkari, M., "Elastic Stability and Dynamic Analysis of Hyperboloidal Shells of Revolution," Thesis presented to the University of Southern California, at Los Angeles, Calif., in 1971; in partial fulfillment of the degree of Doctor of Philosophy.

5. Sanders, J. L., Jr., "Nonlinear Theories for Thin Shells" Quarterly of Applied Mathematics, Vol. 21, No. 1 (1963) pp. 21-36.

6. Kraus, H., Thin Elastic Shells, John Wiley and Sons, Inc., New York, N. Y., 1967.

7. Tajimi, H., "A Statistical Method of Determining the Maximum Response of a Building Structure During an Earthquake," Proceedings of the Second World Conference on Earthquake Engineering, Vol. 2, Japan, 1960.

TABLE 1. EXPERIMENTAL RESULTS ON THE NATURAL FREQUENCIES OF THE HYPERBOLOID WITH ENDS CLAMPED

Natural Frequencies in Cycles Per Second									
n	m = Meridional Wave Number								
	1	2	3	4	5	6	7	8	9
1	---	---	---	---	---	---	---	---	---
2	---	---	---	---	---	---	---	---	---
3	---	1124	---	---	---	---	---	---	---
4	1766	1068	1400	---	---	---	---	---	---
5	---	1278	---	---	2220	---	---	---	---
6	---	1562	1254	1454	---	---	---	---	---
7	---	---	1468	---	1734	---	2670	---	---
8	---	---	---	1616	---	---	---	3066	---
9	---	---	---	1926	2456	---	2816	---	---
10	---	---	---	---	---	---	3550	---	4044

n = Circumferential Wave Number

TABLE 2. THEORETICAL RESULTS ON THE NATURAL FREQUENCIES OF THE HYPERBOLOID WITH FIXED-FREE SUPPORT CONDITIONS

Natural Frequencies in Cycles Per Second						
n	m = Meridional Wave Number					
	1	2	3	4	5	6
1	1274	1967	4572	5370	6135	---
2	1148	779	2367	3830	4959	---
3	1670	528	932	2246	3376	---
4	1842	760	565	1378	2264	---
5	2093	1221	640	928	1617	---
6	2356	1638	1112	771	1337	1941
7	2671	2014	1479	925	1336	1915
8	3093	---	1685	1107	1577	2184

n = Circumferential Wave Number

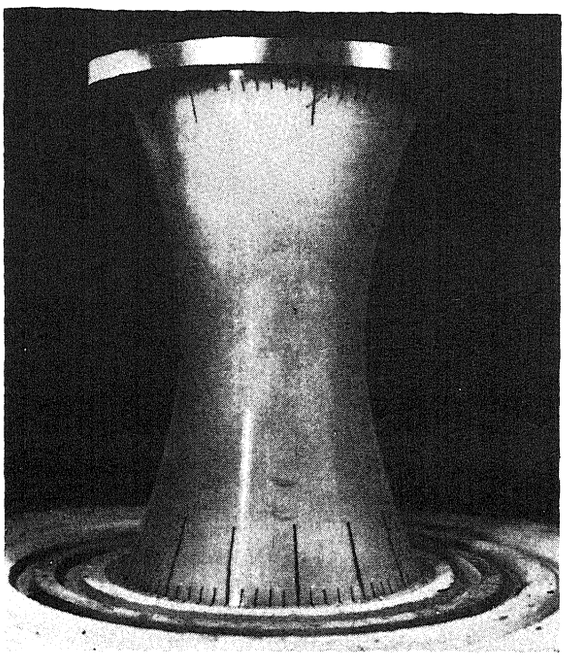

FIG. 1. HYPERBOLOIDAL SHELL SPECIMEN

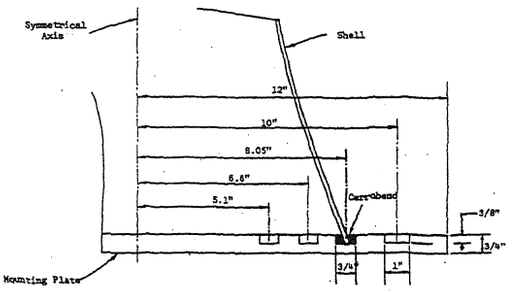

FIG. 2. DETAIL OF SHELL SPECIMEN CLAMPED MOUNTING

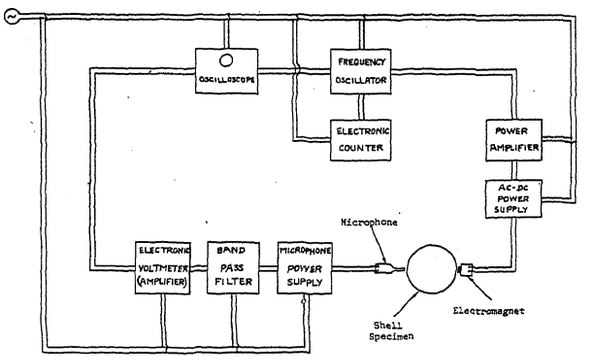

FIG. 3. EXPERIMENTAL SET-UP

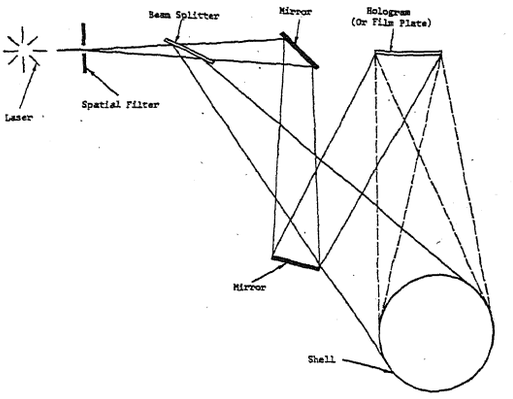

FIG. 4. SET-UP FOR HOLOGRAPHIC INTERFEROMETRY TESTING OF THE HYPERBOLOID

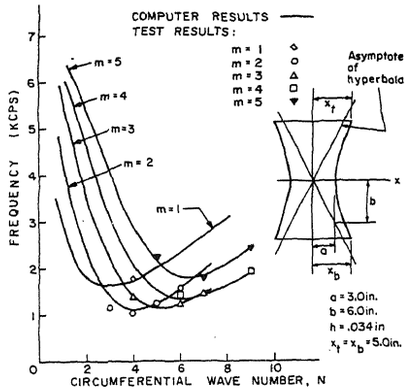

FIG. 5. FREQUENCY VERSUS CIRCUMFERENTIAL WAVE NUMBER, CLAMPED-CLAMPED HYPERBOLOID

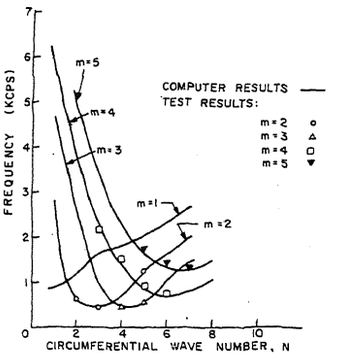

FIG. 6. FREQUENCY VERSUS CIRCUMFERENTIAL WAVE NUMBER, CLAMPED-FREE HYPERBOLOID

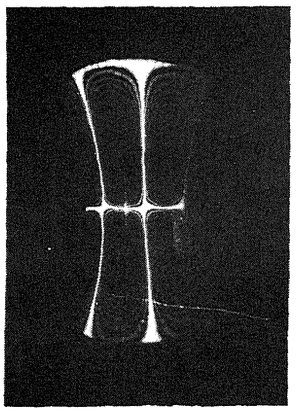

FIG. 7. MODES OF VIBRATION OF HYPERBOLOIDAL SHELL; CLAMPED-CLAMPED, f=1066 Hz, n=4, m=2

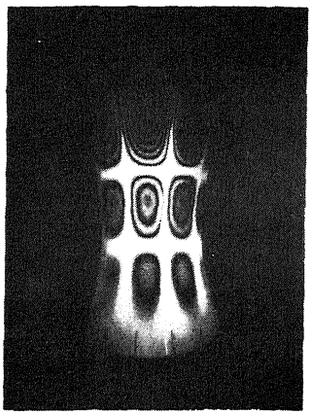

FIG. 8. MODES OF VIBRATION OF HYPERBOLOIDAL SHELL; CLAMPED-FREE, f=550 Hz, n=5, m=3

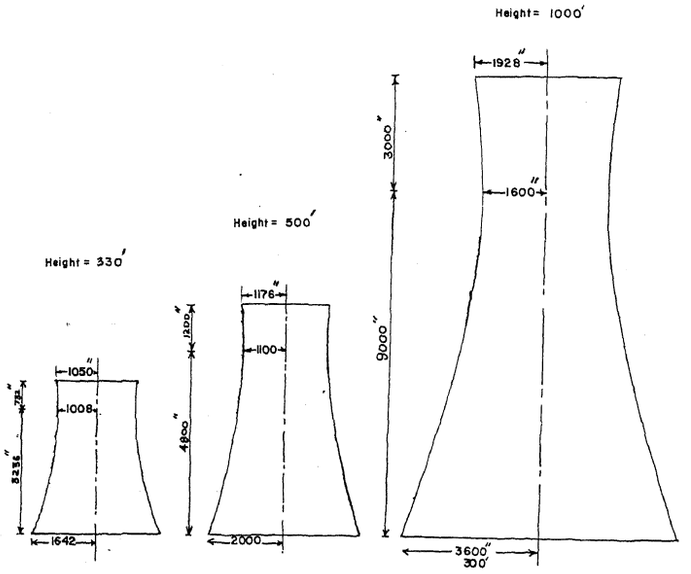

FIG. 9. GEOMETRY OF TYPICAL COOLING TOWERS

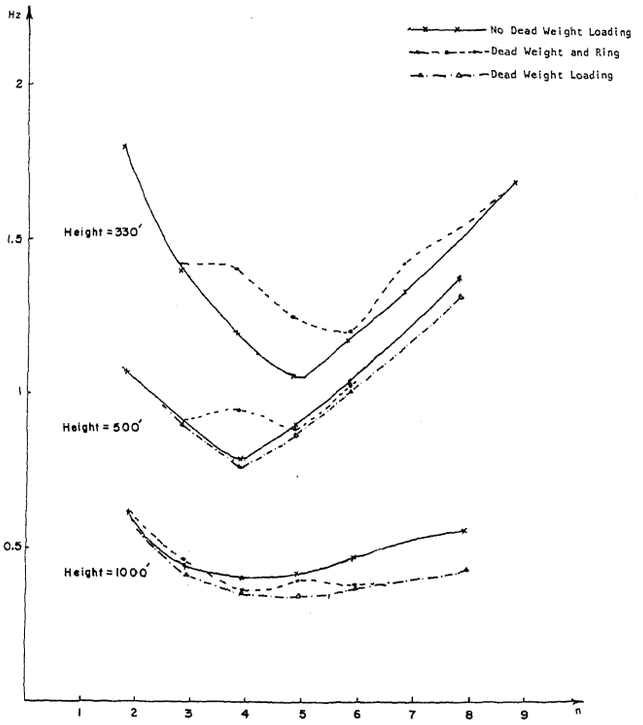

FIG. 10. EFFECTS OF DEADWEIGHT LOADING ON NATURAL FREQUENCIES OF HYPERBOLOIDAL SHELLS

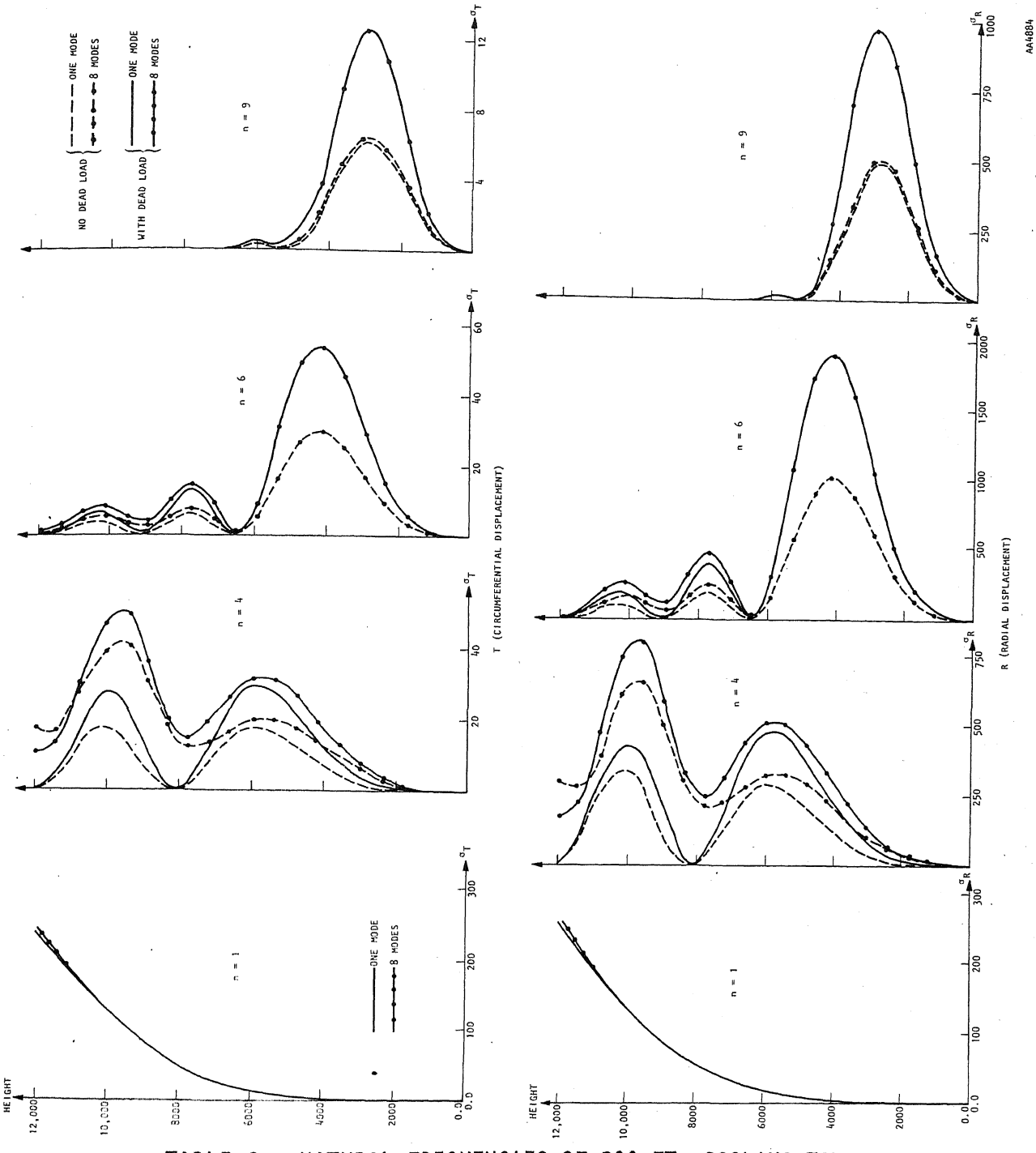

FIG. 11. EFFECTS OF DEADWEIGHT LOADING AND NUMBER OF MODES ON EARTHQUAKE RESPONSE OF HYPERBOLOIDAL SHELLS

TABLE 3. NATURAL FREQUENCIES OF 300 FT. COOLING TOWER

N	Finite Difference Method (3)				Finite Element Method			
	Isotropic		Ring stiffened	% increase due to ring	Isotropic		Ring stiffened	% increase due to ring
	1st Mode	2nd Mode	1st Mode	1st Mode	1st Mode	2nd Mode	1st Mode	1st Mode
1	3.335	6.882	3.382	1.20	3.286	6.786	3.287	0.0
3	1.393	2.015	1.419	2.0	1.375	1.993	1.398	1.6
4	1.200	1.460	1.390	15.9	1.181	1.449	1.380	14.4
5	1.044	1.442	1.197	14.7	1.034	1.431	1.226	15.7
6	1.154	1.334	1.154	0.0	1.148	1.327	1.17	2.0
7	1.306	1.519	1.384	6.1	1.303	1.515	1.389	6.0
9	---	---	---	---	1.651	2.056	1.651	0.0